Scientific Journals
Maritime University of Szczecin

Zeszyty Naukowe
Akademia Morska w Szczecinie

2009, 18(90) pp. 48–53

2009, 18(90) s. 48–53

GNSS signal error part determination for satellite based navigation within maritime high precision applications

Błąd sygnału satelitarnego GNSS w systemach precyzyjnej morskiej nawigacji satelitarnej

A. Hirrle, E. Engler

DLR Institute of Communications and Navigation, Neustrelitz, Germany

Key words: satellite systems, signal processing

Abstract

For satellite based navigation within maritime applications, the IMO defines requirements for further GNSS systems (IMO, 2002). In order to meet e.g. the demands for automatic docking (absolute accuracy: 0.1 m horizontal, integrity: 0.25 m Alert Limit, 10 s Time to Alarm, 10E–5 Integrity Risk (per 3 h), accurate code and phase measurements are essential. As these measurements are distorted by effects of various error sources, efficient error detection and correction are of main interest. This paper presents the idea of describing the influence of error sources in both, time and frequency domain to derive a competent basis for evaluating the signal's quality and detecting outliers. This offers a fundament for signal classification (usable, unusable), prediction of signal states and error correction and thus the compliance with the given requirements. First a description of the used analysis method, the Hilbert Huang Transform is given. By means of data recorded at Tromsoe/Norway and Rostock/Germany, first results are discussed.

Słowa kluczowe: systemy satelitarne, przetwarzanie sygnałów

Abstrakt

Nawigacja satelitarna używana na statkach morskich musi spełniać wymagania określone przez Międzynarodową Organizację Morską [1]. Dokładne kodowanie oraz pomiar faz są niezbędne do spełnienia wymagań np. automatycznego dokowania (całkowita dokładność: 0,1 m w poziomie, integralność: 0,25 m wartość do zgłoszenia alarmu (*Alert Limit*), 10 s – czas do zgłoszenia alarmu (*Time to Alarm*), 10E–5 – ryzyko wiarygodności (*Integrity Risk*) – na 3 h. Pomiary te zniekształcone są poprzez działanie różnych źródeł błędów. Główne zainteresowanie skupia się na skutecznym wykrywaniu i korekcji tych błędów. W artykule przedstawiono ideę opisującą wpływ źródeł błędów w domenach czasu i częstotliwości w celu uzyskania właściwej podstawy do oceny jakości sygnału i wykrywania wartości nietypowych. Umożliwia to stworzenie podstaw do klasyfikacji sygnału (użyteczny, nieużyteczny), przewidywania stanów sygnału i korekcji błędów, a tym samym zgodność ze stawianymi wymogami. W pierwszej części artykułu przedstawiona została transformacja Gilberta Huang oraz zaprezentowano pierwsze wyniki na podstawie danych zarejestrowanych w Tromsoe (Norwegia) i w Rostoku (Niemcy).

Introduction

The paper concentrates on the characterisation of ionosphere induced signal variations and on the signal variations caused by multipath propagation effects. For this reason high-rate (20–50 Hz) dual frequency GPS code and phase measurements have been analysed. The first data sets used for this study, have been recorded in Tromsoe (Norway) during the so called "Halloween Storm", a severe ionospheric storm (Dst-Index up to – 383 nT, [2]) occurred from 29th October to 31st October 2003, and under nearly unperturbed conditions on 7th November, 2003.

The second data sets have been recorded in the port environment of Research Port Rostock on 30th January and 31st January 2007. As the receiver has been set close to a ferry terminal (fig. 1) signals

of satellites in low elevations are influenced by multipath propagation effects.

Fig. 1. Test and measurement car at ferry terminal in Research Port Rostock. In the background a ferry is docking
Rys. 1. Samochód z aparaturą pomiarową na terminalu promowym w porcie Rostok. W tle dokujący prom

The next chapter will introduce in the used analysis method, the Hilbert Huang Transform. Chapter 3 will describe the analysed signals and present first results.

Hilbert Huang Transform Basics

The Hilbert Huang Transform was published in 1998 [3]. It combines the Empirical Mode Decomposition (EMD) and the Hilbert Transform (HT). First the EMD decomposes the original signal in magnitude and frequency varying exponentials, so called Intrinsic Mode Functions" (IMFs), via a sifting process. In a second step the instantaneous frequencies of these mono-components are extracted by HT.

Empirical Mode Decomposition

The base of this decomposition is the assumption, that the signal is a superposition of a finite number of monochromatic oscillations, whereas they may vary in magnitude and frequency over time. These oscillations are called Intrinsic Mode Functions (IMF). In order to be monochromatic an IMF has to fulfil to properties:

1) the IMF has zero local mean.
2) the function has exactly one zero between any two consecutive local extremes.

Within the following iterative algorithm (fig. 2, top) the signal is decomposed in its IMFs, whereas the extraction of an IMF is realized as described in (fig. 2, bottom).

It has already been shown, that the EMD operates as filter bank [4]. First the higher frequent parts are extracted, followed by IMFs with lower frequencies. The last IMF represents the trend. Fig. 3 shows an example.

The original signal (top) is decomposed in 10 IMFs by the method. These IMFs are also represented in figure 3 (bottom). The IMFs are sorted from top to bottom in the order how they were extracted. As it can be seen, the first extracted IMF (top) is the highest frequent component, followed by less frequent IMFs. The last extracted IMF (bottom) represents the trend.

Hilbert Transform

After having decomposed the signal in its IMFs, in the second part of the Hilbert Huang Transform the instantaneous frequencies and their magnitudes

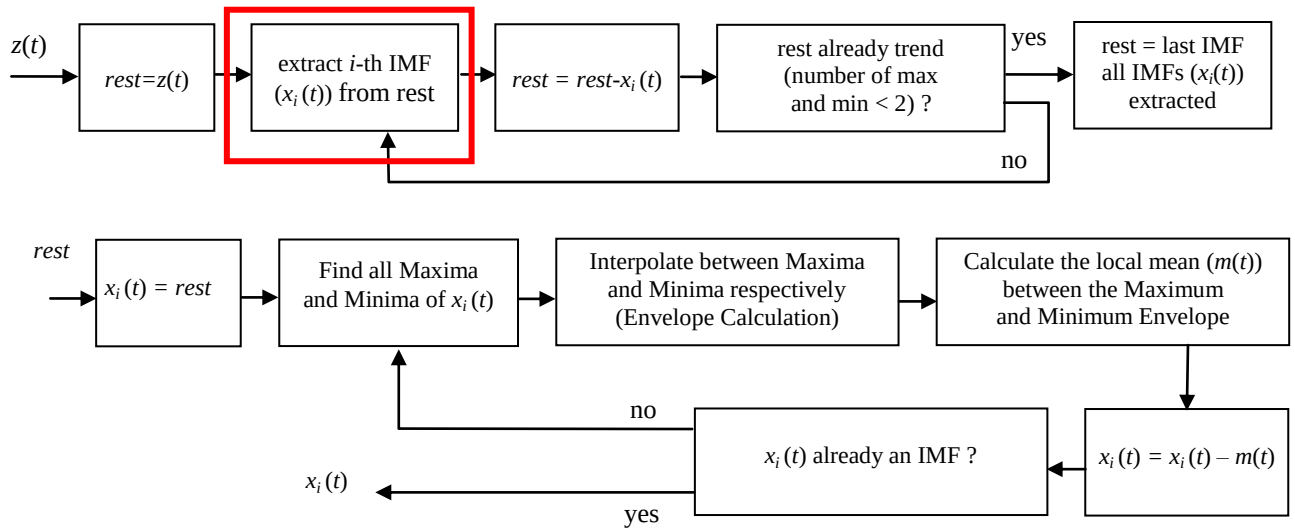

Fig. 2. EMD–Algorithm (top) and Algorithm of IMF Extraction (bottom, red box on top)
Rys. 2. Algorytm EMD (na górze) oraz algorytm IMF Extraction (na dole i zaznaczony kwadrat na górze)

are determined. Therefore for each IMF $x_i(t)$ an analytic signal $z_i(t)$ is created, with the IMF as real part and the IMF's Hilbert Transform $H(x_i(t))$ as imaginary part. This analytic signal has a spectrum equal to zero for negative frequencies and fits with the spectrum of the IMF for positive frequencies. By evaluating the phasor information of the analytic signal, the IMF's instantaneous frequency $\omega_i(t)$ and its magnitude $a_i(t)$ can be calculated.

$$z_i(t) = x_i(t) + jH(x_i(t)) = a_i(t)e^{j\omega_i(t)}$$

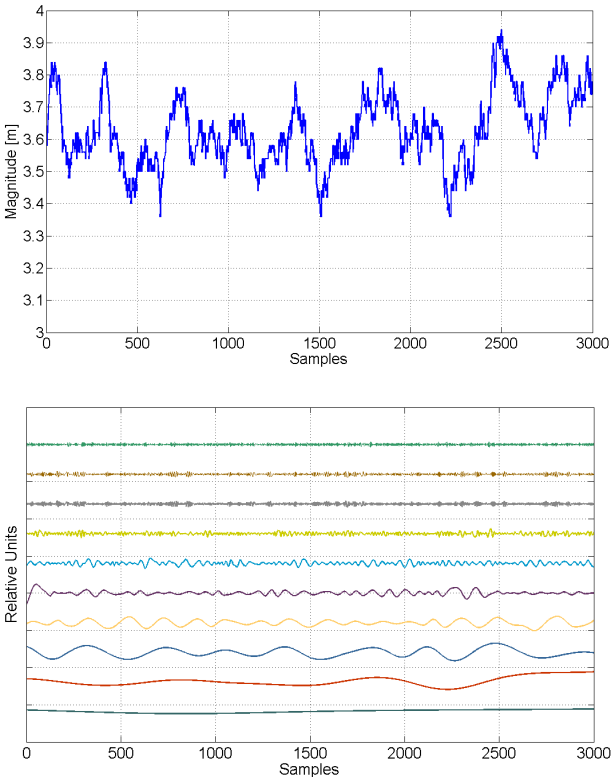

Fig. 3. Example of a signal (top) and its IMFs (bottom). The IMFs are shifted for a better representation since they are all zero-mean (except the trend)
Rys. 3. Przykład sygnału (na górze) oraz jego IMF (na dole). IMF zostały przesunięte w celu lepszego przedstawienia (z wyjątkiem trendu)

Data analysis results

Ionospheric influence

In order to describe the ionospheric influence on the data, the interfrequency difference of the phase measurements on L1 and L2 [m] has been analysed. This interfrequency difference consists of a constant term C_L, the interfrequency ionospheric delay difference (I_2–I_1), the interfrequency multipath difference (δm_2–δm_1) and measurement noise (ε_2–ε_1) [5].

$$L_2(t) - L_1(t) \approx C_L - \{I_2 - I_1\} + \{\delta m_2 - \delta m_1\} + \varepsilon_2 - \varepsilon_1$$

First of all general information of the energy of each IMF and the frequency of each IMF are collected. These information shall be used for a description of the regular behaviour of the L2-L1--difference as function of e.g. elevation. In order to provide a large data base, the L2-L1-difference has been calculated for every satellite. Next the difference has been split in one minute intervals and decomposed afterwards. For these intervals the energy and frequency values of each IMF have been analysed. For all these values the median frequency, median period and median energy per IMF have been determined. As a result a description of the regular behaviour of L2-L1-difference can be derived and outliers can be detected. For first analyses data recorded on 3 days, 30th and 31st October 2003 and 7th November 2003 in Tromsoe/ Norway during and shortly after high ionospheric activities have been used.

As an example, the data of the 31st October are presented and the elevation dependency is analysed. The results are shown in figure 4.

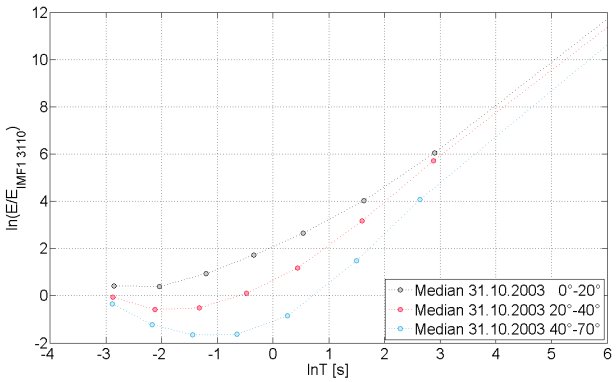

Fig. 4. Median Energy as a function of Median Period of an IMF depending on the elevation, 31st October, decomposition in 8 IMFs. The values of the last IMF are not plotted. The energy is normalized on the median energy of the first IMF calculated from the data of all elevations on 31st October 2003
Rys. 4. Średnia energia jako funkcja średniego okresu IMF w zależności od wzniesienia, 31 października, rozkład na 8 IMF. Wartości ostatniego IMF nie zostały naniesione na rysunek. Energia jest znormalizowana w środkowej energii pierwszego IMF, obliczone na podstawie danych dla wszystkich wzniesień 31 października 2003 r.

For all IMFs it can be stated that the lower the elevation the higher the energy. This results from the fact that the propagation path is longer in lower elevations and that's why the influence of ionosphere and multipath is stronger. Additionally it is to be seen, that in high elevations the energy is decreasing in the first IMFs (hence behaves like white noise [4, 6] and increasing in the last IMFs, whereas in low elevations (expect for the first IMF) the energy is increasing from IMF to IMF for all IMFs. This may be explained by the fact, that in

high elevations multipath effects can be excluded and only the ionospheric influence (considered as low frequent) and measurement noise are left. In low elevations multipath effects are present and interfere with the ionospheric effects. The results remain the same for all the other days. Due to the fact, that the data on 30th October were recorded during strong disturbed ionospheric conditions, whereas the ionosphere on 31st October calmed down and was nearly unperturbed on 7th November it is attended, that there is at least a difference between the median energy of the IMFs on different days. Fig. 5 shows the elevation independent results. The median energy of the first two IMFs as well as the median energy of the last three IMFs (without trend) is increased on 30th October, especially the latter. A second effect is the difference in the median period of the last IMFs. It is higher on the perturbed 30th October.

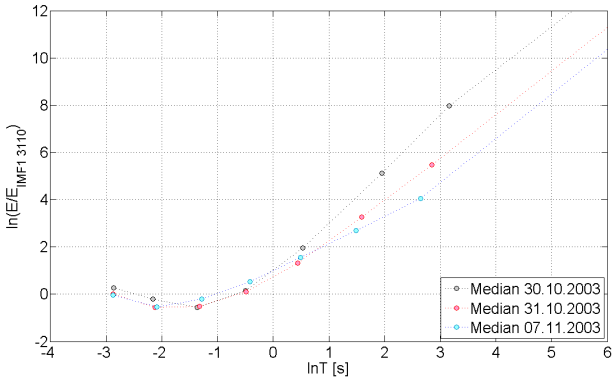

Fig. 5. Median Energy as a function of Median Period of an IMF depending on the day, decomposition in 8 IMFs, elevation independent. The values of the last IMF are not plotted. The energy is normalized on the median energy of the first IMF calculated from the data on 31st October
Rys. 5. Średnia energia jako funkcja średniego okresu IMF w zależności od dnia, rozkład na 8 IMF, wzniesienie niezależne. Wartości ostatniego IMF nie zostały naniesione na rysunek. Energia jest znormalizowana w środkowej energii (lub o średniej energii) pierwszego IMF, obliczone na podstawie danych z 31 października 2003 r.

Since a median value itself does not provide enough information concerning conclusion on normal behaviour and detection of outliers, additionally 2-dimenional Box-and-Whisker-Structures were calculated for the median values of period and energy of a certain decomposition number. They provide a basis for decision to detect outlier.

As an example, figure 6 presents the Box-and-Whisker-Structure calculated from all minutes decomposed in 8 IMFs on 7th November 2003 in an elevation between 40 and 70° (fig. 6). The black stars mark the median period-median energy values of a particular IMF; the black box contains 50% of the values of a particular IMF; the coloured boxes mark the 1.5-Whisker (e.g. IMF 7: median value: lnT = 2.3, lnE = 2.3, 50%-box: lnT = 1.9…3.3, lnE = 1.0…4.5, 1.5-Whisker-Box: lnT = 1.4…5.5 lnE = –1.2…5.5).

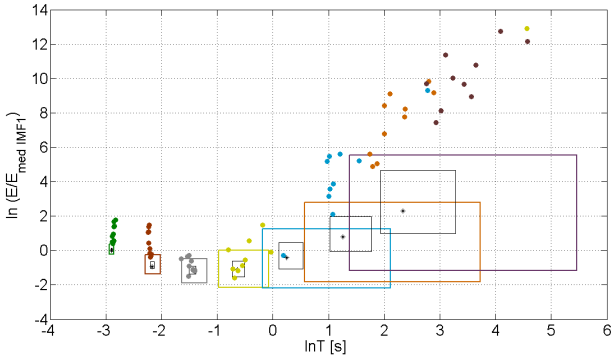

Fig. 6. 2-dimensional-Box-and-Whisker for IMFs 1 to 7 calculated from all minutes decomposed in 8 IMFs on 7th November 2003 in an elevation between 40 and 70°. The dots present the minute intervals with ionospheric signatures on 30th October 2003 between 21:00 and 22:00 UTC of satellite with PRN 18
Rys. 6. Dwuwymiarowy wykres typu „Box-and-Whisker" dla IMF od 1 do 7, uwzględniając wszystkie minuty rozłożone na 8 IMF, 7 listopada 2003 r., na wysokości pomiędzy 40 i 70°. Kropki przedstawiają odstępy minutowe z oznaczeniami jonosferycznymi, 30 października 2003 r., pomiędzy 21:00 a 22:00 czasu UTC, dla satelity PRN 18

Next, the IMFs' median energy values and median period values of all minute intervals appearing during the occurrence of ionospheric effects are compared with these Box-and-Whisker-structures. As an example the IMFs' median period and energy values of the minute intervals from 21:25 to 21:50 (UTC) of satellite with PRN 18 (all decomposed in 8 IMFs) are plotted as coloured circles (fig. 6). As it can be seen the energy values of nearly all IMFs are outside the 1.5-Whisker on 30th October (coloured dots) during the occurrence of strong ionospheric effects.

Multipath Propagation Influence

In order to describe the multipath propagation influence on the data, the code-carrier-difference C1 and L1 [m] has been analysed. This difference consists of a constant term C_{CL}, two times the ionospheric delay ($2I_1$), the multipath delay difference (δm_1–dm_1) and measurement noise (ε_1–e_1) [5].

$$L_1(t) - C_1(t) \approx C_{CL} - 2I_1 + \{\delta m_1 - dm_1\} + \{\varepsilon_1 - e_1\}$$

The analysis procedure remains the same as for the L2-L1-Difference. First the code-carrier--difference has been calculated for every satellite. Next the difference has been split in one minute intervals and decomposed afterwards. For these

intervals the energy and frequency values of each IMF have been analysed. For all these values the median frequency, median period and median energy per IMF have been determined. As a result a description of regular behaviour of the code--carrier-difference can be derived and outliers can be detected. For first analyses data recorded on 2 days, 30th and 31st January 2007 in Rostock/ Germany in a port environment next to a ferry terminal have been used. As an example, the data of the 30th and 31st October are presented and the elevation dependency is analysed. The results are shown in figure 7.

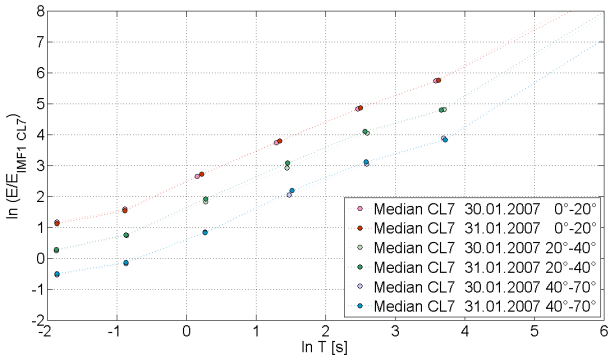

Fig. 7. Median Energy as a function of Median Period of an IMF depending on the elevation, 30th and 31st January, decomposition in 7 IMFs. The values of the last IMF are not plotted. The energy is normalized on the median energy of the first IMF calculated from the data of all elevations

Rys. 7. Średnia energia jako funkcja średniego okresu IMF w zależności od wzniesienia, 30 i 31 stycznia, rozłożone na 7 IMF. Wartości ostatniego poziomu IMF nie zostały naniesione. Energia jest znormalizowana w środkowej energii (lub o średniej energii) pierwszego poziomu IMF obliczonego dla wszystkich danych wzniesień

For all IMFs it can be stated that the lower the elevation the higher the energy. This results from the fact that the propagation path is longer in lower elevations and that's why the influence of ionosphere and multipath is stronger. The results for the two analysed days are almost the same. Hence the presented relation can be seen as reference and base for outlier detection.

Similar to the outlier detection procedure for the L2-L1-Difference a 2-dimensional Box-and-Whisker-Structure is calculated. As an example, Fig. 8 presents the Box-and-Whisker-Structure calculated from all minutes decomposed in 7 IMFs on 31st January 2007. The black stars mark the median period-median energy values of a particular IMF; the black box contains 50% of the values of a particular IMF; the coloured boxes mark the 1.5-Whisker. Next, the IMFs' median energy values and median period values of all minute intervals are compared with these Box-and-Whisker-structures. As an example the IMFs' median period and energy values of the minute intervals from 18:09 to 18:15 (UTC) of satellite with PRN 11 (all decomposed in 7 IMFs) are plotted as coloured triangles (30th January 2007) and coloured circles (31st January 2007), respectively. On 31st January during these minutes the signals where highly disturbed due to a docking ferry. As it can be seen the median values of almost all IMFs are outside the 1.5-Whisker.

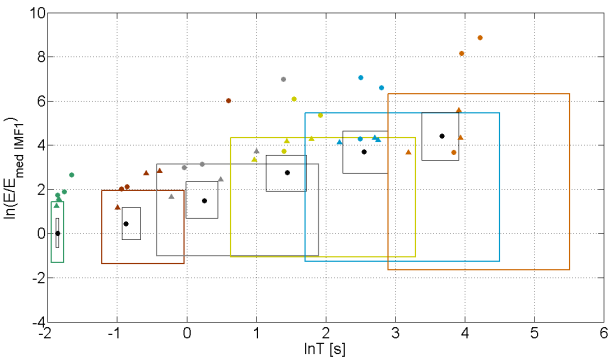

Fig. 8. 2-dimensional-Box-and-Whisker for IMFs 1 to 6 calculated from all minutes decomposed in 7 IMFs on 31st January 2007. The dots present the minute intervals with strong multipath signatures on satellite with PRN 11 on 31st October 2007 between 18:09 and 18:15. The triangles represent the values of these minutes on 30th October 2007

Rys. 8. Dwuwymiarowy wykres typu „Box-and-Whisker" dla poziomów IMF od 1 do 6, obliczony dla wszystkich minut rozłożonych w poziomach 7 IMF, 31 stycznia 2007 r. Kropki przedstawiają odstępy minutowe o silnym „podpisie" wielościeżkowym na satelitę PRN 11, 31 października 2007 r., pomiędzy 18:09 a 18:15. Trójkąty na wykresie określają wartości tych minut na 30 października 2007 r.

Conclusions

In order to meet the IMO-requirements for automatic docking with GNSS, accurate code and phase measurements are essential. As these measurements are distorted by effects of various error sources, efficient error detection and correction are of main interest. For this purpose high rate GNSS measurement data (20/50 Hz) have been analysed with Hilbert Huang Transform. As a result reference behaviour has been determined and outlier detection has been realized. Further work aim on using a larger data base to validate the reference and on evaluating the procedure of outlier detection.

References

1. IMO (2002), IMO Resolution A. 915(22), Appendix 3.
2. Kyoto: World Data Centre for Geomagnetism, Kyoto, http://wdc.kugi.kyoto-.ac.jp/dst_final/f/dstfinal-200310.html, 2009.

3. HUANG N.E. ET AL.: The empirical mode decomposition and the Hilbert spectrum for nonlinear and non-stationary time series analysis. Proc. R. Soc. Lond. A, Vol. 454, 1998, 903–995.
4. FLANDRIN P., RILLING G., GONCALVÉS P.: Empirical Mode Decomposition as a Filter Bank. IEEE Signal Processing Letters, Vol. 11, No. 2, 2004, 112–114.
5. TEUNISSEN P.J.G., KLEUSBERG A.: GPS for Geodesy. Springer Verlag, 1998.
6. WU Z., HUANG N.E.: A study of the characteristics of white noise using the empirical mode decomposition method, Proc. R. Soc. Lond. A, Vol. 460, 2004, 1597–1611.

Recenzent:
prof. dr hab. inż. Bolesław Mazurkiewicz
Akademia Morska w Szczecinie